

# Surface plasma wave in spin-polarized semiconductor quantum plasma

Punit Kumar and Nafees Ahmad 

Department of Physics, University of Lucknow, Lucknow 226007, India

## Letter to the Editor

**Cite this article:** Kumar P, Ahmad N (2020). Surface plasma wave in spin-polarized semiconductor quantum plasma. *Laser and Particle Beams* **38**, 159–164. <https://doi.org/10.1017/S026303462000018X>

Received: 16 March 2020  
Revised: 5 May 2020  
Accepted: 5 May 2020  
First published online: 27 May 2020

### Key words:

QHD model; quantum plasma; spin-polarization; surface plasma wave

### Author for correspondence:

Nafees Ahmad, Department of Physics,  
University of Lucknow, Lucknow 226007, India.  
E-mail: [plasmalu2018@gmail.com](mailto:plasmalu2018@gmail.com)

## Abstract

The possibilities of surface plasma wave (SPW) on a metal-vacuum interface in semiconductor quantum plasma by considering the effects of Coulomb exchange (CE) interaction and the spin-polarization has been explored. The dispersion for the SPW has been setup using the modified quantum hydrodynamic (QHD) model taking into account the Fermi pressure, the quantum Bohm force, the CE, and the electron spin. The optical gain of SPW has been evaluated. It is found that CE effects and spin-polarization increases the wave frequency and enhances the gain during the stimulated emission.

## Introduction

The propagation of surface waves at the boundary between two media with different conductivities and dielectric properties has been an important area of research over the past many years. A surface plasma wave (SPW) is a guided electromagnetic mode which propagates between a conductor and a dielectric (Agranovich, 1975; Liu and Tripathi, 2000; Zayats *et al.*, 2005; Kumar *et al.*, 2008; Goel *et al.*, 2016). The SPW is excited due to collective oscillations of free electrons at the interface and its field decays exponentially away from the interface, the dielectric, as well as into the conductors. The characteristics of these modes have been extensively studied in plasmas due to their special frequency spectrum (Trivelpiece and Gould, 1959). The presence of small traces of a material on the interface brings a considerable change in characteristics of SPW and this feature is of great importance to bio and nanoparticle sensors (Homola, 1999, 2003; Kao *et al.*, 2003; Hong and Kao, 2004), micro-optics (Bozhevolnyi and Pudonin, 1997), and development of nanolaser. SPW plays an important role in metamaterials (Ishimaru *et al.*, 2005) that effectively have a negative refractive index.

Due to the great degree of miniaturization of semiconductors in electronic devices, the thermal de Broglie wavelength of charged particles can be now comparable to the spatial variation of the doping profile. Thus, the typical quantum effects such as the exchange-correlation, the quantum fluctuation due to the density correlation, and the degenerate pressure will play a significant role in the electronic components to be constructed in future. In the previous investigations (Ritchie, 1963; Kaw and McBride, 1970; Lazar *et al.*, 2007; Mohamed, 2010; Misra, 2011; Zhu, 2015), the basic features of the surface waves in semi-bounded plasmas have been investigated under the influence of the quantum tunneling (Shahmansouri, 2015; Moradi, 2017), relativistic effects (Zhu *et al.*, 2013), spin fermions (Andreev and Kuzmenkov, 2016), the collisional effects (Khorashadizadeh *et al.*, 2012), exchange effects (Shahmansouri, 2015; Moradi, 2017; Shahmansouri and Mahmodi, 2017), as well as the external magnetic field (Mohamed, 2010).

Quantum effects are significant in the transport of electrons in normal metals and electron and holes in semiconductors. The effects of quantum tunneling and quantum degeneracy pressure, which arise due to Heisenberg's uncertainty principle and Pauli's exclusion principle in the electron-hole quantum semiconductors, have been studied by several authors. In semiconductor quantum plasmas, the charge carriers obey the Fermi-Dirac distribution instead of Maxwell-Boltzmann distribution. Recently, advanced laser technology has provided excellent opportunities to construct powerful laser pulses (Yanovsky *et al.*, 2008). Interactions between short laser pulses with the matter may allow the creation of electron-hole (e-h) plasmas at high densities (Shukla and Eliason, 2007). In recent miniature semiconductor structures, the characteristic space scales of impurity variations are comparable to the characteristic electron and hole de Broglie thermal wavelengths. When a semiconductor is excited by a short laser pulse, electrons absorb the photon energy and transit from the valence band to the conduction band via single- and or multi-photon absorption, depending on the photon energy and the band gap energy. This interband transition of the electrons creates holes in the valence band and this state may satisfy the plasma conditions. For semiconductor quantum devices working with the electrons and holes in nanoscale sizes, it is essential to understand and investigate thoroughly the quantum mechanical effects on the dynamics of the charge carriers.

Spin plasma physics was developed from the Pauli-Hamiltonian formulation and generalization of the Madelung decomposition for the two-component spinor wave function. In

strong magnetic fields, the electron spin plays an important role. Collective spin effects can influence the wave propagation in strongly magnetized quantum plasma (Brodin and Marklund, 2007a, 2007b, 2007c). The electron spin-1/2 is an intrinsic property of electrons having an intrinsic angular momentum characterized by quantum no. 1/2 and magnetic moment of individual electrons. The evolution of intrinsic spin effect of electrons is one of the most important properties of quantum plasma, and it may survive even when the macroscopic variations occurs on a scale larger than the thermal de Broglie wavelength. For high-density plasma, quantum features due to the intrinsic magnetic moment of the electron become noticeable and their spin effect (Polyakov, 1979; Marklund and Brodin, 2007; Brodin and Marklund, 2008) in plasma are found to be somewhat different from those of non-spin (Rastunkov and Krainov, 2004; Manfredi, 2005) quantum effects in plasma. During the last decade, there have been many papers devoted to the influence of spin-1/2 effect on dynamics of plasma (Shahid *et al.*, 2012; Hu *et al.*, 2016). Previous studies in quantum plasma have been performed taking the macroscopic average of the electron spin. The electron spin has been taken to be average spin-1/2, which is the violation of Pauli's exclusion principle. Moreover, the interaction between spin-up and spin-down electrons has not been accounted for.

In the present paper, we propose a scheme of stimulated SPW excitation via stimulated electron-hole recombination in the proximity of the guiding surface. We consider a three-layer system: a thin layer of n-type semiconductor sandwiched between a metal and p-type semiconductor. The p-n junction is forward biased and is within a few microns from the metal surface where SPW is guided. The mechanism of optical gain of the SPW field encompasses the p-n junction. The SPW field stimulates electron-hole recombination producing surface plasmons. The enhanced SPW field induces stronger e-h recombination, thus exponentiating the growth of SPW in the initial stage of instability.

We have used the recently developed quantum hydrodynamic (QHD) model incorporating the Fermi pressure, Bohm potential, and spin magnetic moment. The advantages of this model over kinetic ones are the numerical efficiency, the direct use of macroscopic variables of interest, such as momentum and energy, and the easy way the boundary conditions are implemented. This allows to consider the nonlinear phenomena relatively easier and so this model approach is preferred for describing such phenomena in quantum plasma. The spin-up and spin-down electrons have been taken to be two independent particle species

and the interaction between the two spinning electrons have been taken into account. Initially, the two spinning species have equal concentration. The interaction of high-intensity e.m. wave with the high-density quantum plasma under the influence of strong magnetic field induces a difference in concentration of spin-up and spin-down electrons leading to spin-polarization. Such a study on SPW on the metal surface with spin-polarization (produced under the influence of the external magnetic field) in semiconductor quantum plasma interaction has not been reported in the literature so far.

The interaction of the incident electromagnetic wave with the surface quantum plasma under the influence of the coulomb exchange (CE) interaction force has been developed in the formalism section, and the dispersion relation has been setup which has been analyzed graphically. The gain due to electron-hole recombination has been calculated in the optical gain section. The last section is devoted to a brief summary and discussion of the obtained results.

### Formalism

Consider a multilayered structure (as shown in Fig. 1) with  $x < 0$  as metal,  $0 < x < d$  as n-type semiconductor,  $d < x < d'$  as p-type semiconductor, and  $x > d'$  as vacuum. The p- and n-type semiconductors may belong to the same host material (e.g., GaAs), but doping levels are fairly high so that the hole and electron Fermi levels in the two lie in the conduction and valence band, respectively. The p-n junction has a width  $\Delta$ . The system is embedded in an axially directed external magnetic field  $\vec{B}_0 = b\hat{z}$ .

The set of QHD equations describing the motion of electrons and holes under the influence of electromagnetic fields are as follows (Shahmansouri, 2015; Sahu and Misra, 2017):

$$\frac{\partial \vec{v}_{\alpha j}}{\partial t} = \frac{q_{\alpha j}}{m_j} [\vec{E} + v_{\alpha j} \times \vec{B}_0] - \frac{\nabla P_{\alpha j}}{m_j n_{\alpha j}} + \frac{\hbar^2}{2m_{\alpha j}^2} \nabla \left[ \frac{1}{\sqrt{n_{\alpha j}}} \nabla^2 \sqrt{n_{\alpha j}} \right] + \frac{\nabla V_{\alpha j}}{m_j} + \frac{2\mu}{\hbar} \nabla (\vec{B} \cdot S_{\alpha j}), \quad (1)$$

$$\left( \frac{\partial}{\partial t} + v_{\alpha j} \cdot \nabla \right) S_{\alpha j} = -\frac{2\mu}{\hbar} B \times S_{\alpha j}, \quad (2)$$

and

$$\frac{\partial n_j}{\partial t} + n_{0\alpha j} \nabla \cdot v_{\alpha j} = 0, \quad (3)$$

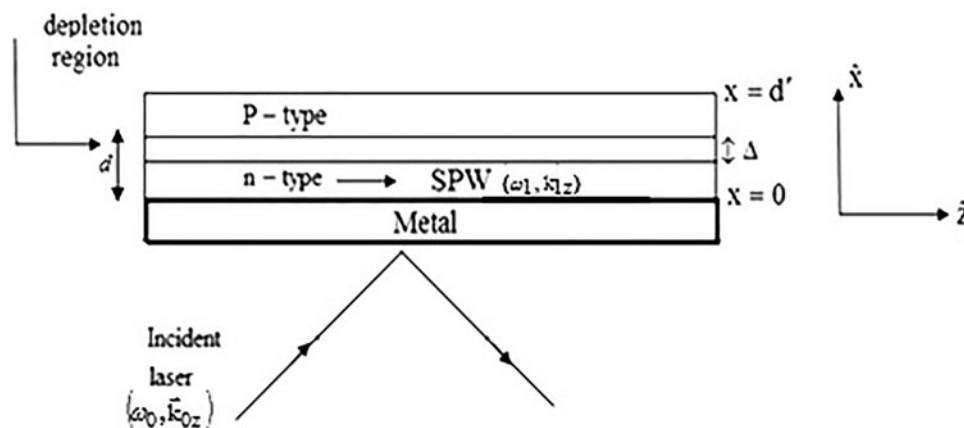


Fig. 1. The systematic structure of semiconductor plasma.

where  $n_{\alpha j}$ ,  $v_{\alpha j}$ , and  $q_{\alpha j}$  are the number density, velocity, and charge of species  $\alpha j$ , respectively. The subscript  $\alpha$  denotes spin-up ( $\uparrow$ ) and spin-down ( $\downarrow$ ) particles, respectively, and subscript  $j$  is for plasma electrons and holes. The first term on the right-hand side of Eq. (1) refers to Lorentz force, the second term is the to degenerate pressure  $P_{\alpha j} = m_j v_{F\alpha j}^2 n_j^{5/3} / 5 n_{0\alpha j}^{2/3}$ , where  $v_{F\alpha j} = \sqrt{\zeta_{3D}} \hbar (3\pi^2 n_{0\alpha j})^{1/3} / m_{\alpha j}$  is the Fermi velocity.  $\zeta_{3D}$  is the degree of spin-polarization given by  $\zeta_{3D} = [(1 - \eta)^{5/3} + (1 + \eta)^{5/3}] / 2$  with spin-polarization ( $\eta$ ) defined by  $\eta = |n_{\uparrow} - n_{\downarrow}| / |n_{\uparrow} + n_{\downarrow}|$ . The third term represents the quantum Bohm potential and the fourth term is the CE interaction force given by  $V_{cj} = 3^{4/3} \pi^{-1/3} v_{3D} e^2 n_{\alpha j}^{4/3} / 4$ , where  $v_{3D} = [(1 + \eta)^{4/3} - (1 - \eta)^{4/3}]$ . The last term is the force due to spin magnetic moment of two different electron species (spin-up and spin-down) of plasma electrons under the influence of the external magnetic field, where  $\mu = e\hbar / 2m$  is the Bohr magneton.

Pertubatively expanding Eq. (1) in orders of the radiation field and solving for the first order of the perturbed velocities gives us,

$$\delta v_{\alpha jx} = [(-e/m_{\alpha j})i/\omega^2 - ikQ_{\alpha j}^2 V_{cj}^2/m_j(\omega^2 - k^2 Q_{\alpha j}^2)]\delta \vec{E}_x,$$

$$\delta v_{\alpha jy} = [(-e/m_{\alpha j})/\omega^2 - k^2 Q_{\alpha j}^2 V_{cj}^2/m_j(\omega^2 - k^2 Q_{\alpha j}^2)]\delta \vec{E}_y,$$

$$\delta v_{\alpha jz} = [(-e/m_{\alpha j})i\omega/(\omega^2 - k^2 Q_{\alpha j}^2) - ieV_{cj}^2/m_j(\omega^2 - k^2 Q_{\alpha j}^2)]\delta \vec{E}_z,$$

where  $Q_{\alpha j}^2 = v_{F\alpha j}^2 + (k^2 v_{F\alpha}^2 / 4\omega_p^2) H_{\alpha}^2$  and  $H_{\alpha} = \hbar \omega_{p\alpha j} / m_j v_{F\alpha}$  is the ratio of electron Plasmon energy to the Fermi energy densities.

The effective relative permittivities of n-type and p-type regions are obtained using the electron and hole current densities ( $J_{\alpha} = \rho_{\alpha j} v_{\alpha j} = \sigma_{\alpha j} \cdot \vec{E}$ ), where  $\sigma_{\alpha j}$  and  $\rho_{\alpha j}$  are the

p-type and n-type semiconductors as a single medium with effective permittivity  $\epsilon_1 \approx \epsilon_{\alpha j}$ .

The plasma density inside the metal will be high enough but will not reach the threshold values for degeneracy, under such conditions the effective permittivity of the metal will be,

$$\epsilon_2 = \epsilon_L - \omega_p^2/\omega^2, \tag{5}$$

where  $\epsilon_L$  is the lattice permittivity of metal.

We assume the SPW fields to vary as  $\exp i(kz - \omega t)$ . The electric and magnetic field of the e.m. wave, consistent with the wave equation and the continuity of  $E_z$  across  $x = 0$ , can be written as follows:

$$\left. \begin{aligned} E_z &= A e^{\alpha_{II} x} e^{i(kz - \omega t)} \\ E_x &= -\frac{ik}{\alpha_{II}} A e^{\alpha_{II} x} e^{i(kz - \omega t)} \\ H_y &= -A \frac{i\omega \epsilon_2}{c\alpha_{II}} e^{\alpha_{II} x} e^{i(kz - \omega t)} \end{aligned} \right\} x < 0 \tag{6}$$

and

$$\left. \begin{aligned} E_z &= A e^{-\alpha_I x} e^{i(kz - \omega t)} \\ E_x &= \frac{ik}{\alpha_I} A e^{-\alpha_I x} e^{i(kz - \omega t)} \\ H_y &= A \frac{i\omega \epsilon_1}{c\alpha_I} e^{-\alpha_I x} e^{i(kz - \omega t)} \end{aligned} \right\} x > 0, \tag{7}$$

where  $\alpha_I = (k^2 c^2 - \omega^2 \epsilon_1 / c^2)^{1/2}$  and  $\alpha_{II} = (k^2 c^2 - \omega^2 \epsilon_2 / c^2)^{1/2}$ . The equations  $\nabla \cdot \vec{E} = 0$  and  $c(\nabla \times \vec{E}) = i\omega \vec{H}$  are valid in each region. Employing the continuity of  $H_y = 0$  across  $x = 0$ , we get  $\epsilon_2 / \epsilon_1 = -\alpha_{II} / \alpha_I$ , leading to the dispersion relation of the SPW:

$$k = \frac{\omega}{c} \left[ \frac{\{\epsilon'_L - \omega_p^2 \omega / (\omega^2 - k^2 Q_{\alpha j}^2) - \omega_p^2 \omega m_j V_{cj}^2 / (\omega^2 - k^2 Q_{\alpha j}^2)\}}{1 + ((\{\epsilon'_L - \omega_p^2 \omega / (\omega^2 - k^2 Q_{\alpha j}^2) - \omega_p^2 \omega m_j V_{cj}^2 / (\omega^2 - k^2 Q_{\alpha j}^2)\}) / (\epsilon_L - \omega_p^2 / \omega^2))} \right]^{1/2}. \tag{8}$$

conductivities and charge densities of respective species. They come out to be,

$$\epsilon_{\alpha j} \cong \epsilon'_L - \omega_p^2 \omega / (\omega^2 - k^2 Q_{\alpha}^2) - \omega_p^2 \omega m_j V_{cj}^2 / (\omega^2 - k^2 Q_{\alpha j}^2), \tag{4}$$

where  $\epsilon'_L$  is the relative permittivity of the lattice,  $\omega_p^2 = [(1 - \eta)\omega_{p\uparrow}^2 + (1 + \eta)\omega_{p\downarrow}^2] / 2$ . We consider  $\epsilon'_L \gg [\omega_p^2 \omega / (\omega^2 - k^2 Q_{\alpha j}^2) - \omega_p^2 \omega m_j V_{cj}^2 / (\omega^2 - k^2 Q_{\alpha j}^2)]$  and take both the

The average Poynting flux of the SPW is given as follows:

$$P_z = c(E_x H_y / 8\pi). \tag{9}$$

The above equation on integration w.r.t.  $x$  in the limit  $-\infty$  to  $+\infty$  gives the power flow of the wave per unit  $y$ -width:

$$I = \frac{c^3 A^2 [2\omega^2 (\omega^2 - k^2 Q_{\alpha j}) - \omega_p^2 \omega^2 - \omega_p^2 V_{cj}^2 (\omega^2 - k^2 Q_{\alpha})]^4 \omega_p^2 (\omega^2 - k^2 Q_{\alpha}) - \omega_p^2 \omega^2}{k^3 \omega^8 (\omega^2 - k^2 Q_{\alpha})^3 Q_{\alpha}^2 (1 - \omega_p^2 / \omega^2)}. \tag{10}$$

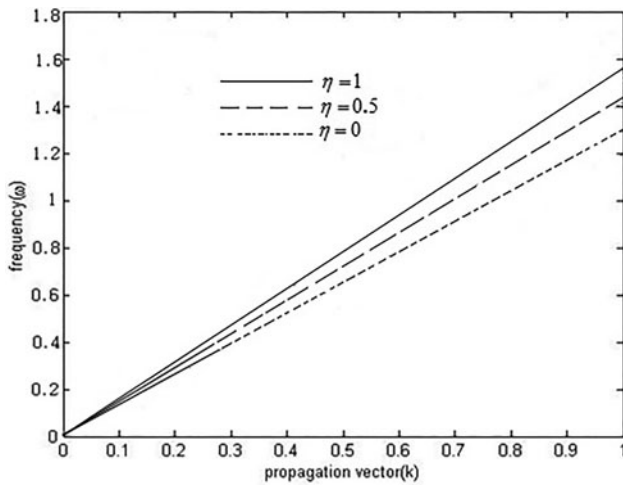
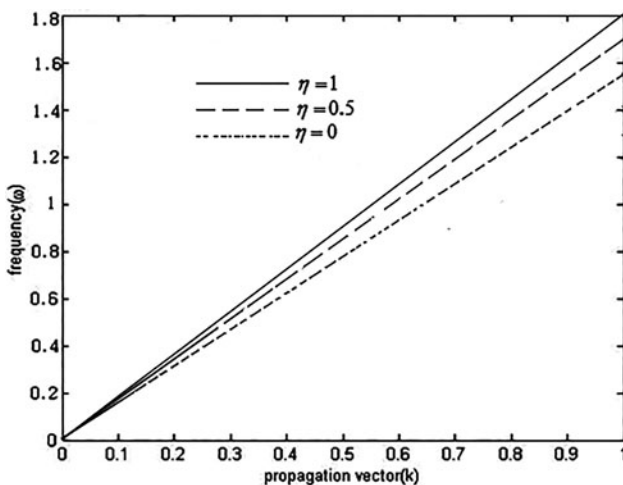


**Fig. 2.** The variation frequency of the SPW ( $\omega$ ) with the propagation vector ( $k$ ) in the absence of CE interaction for the different values of the spin-polarization at  $\eta = 0, 0.5,$  and  $1,$  with  $B_0 = 1\text{T}$  and  $n_{0\alpha} = 10^{26}\text{ m}^{-3}$ .

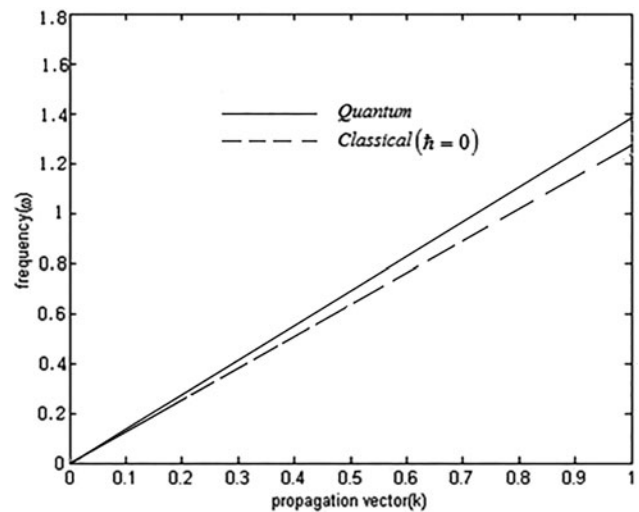
In the numerical analysis to follow, we consider the typical values of physical parameters for which the electrons are degenerate (Shahmansouri and Misra, 2018), namely  $n_{\alpha 0} \sim 10^{26}\text{ m}^{-3}$ . With this choice, the average inter-particle distance  $1/\sqrt[3]{n_{\alpha 0}}$  becomes smaller than the thermal de Broglie wavelength  $\lambda_B$  (i.e.,  $\lambda_B/\sqrt[3]{n_{\alpha 0}} \sim 2.5 > 1$ ), which means that the quantum effects are no longer negligible. The external magnetic field  $B_0 \sim 1\text{T}$ . The normalized frequencies taken are  $\omega_{p\alpha}/\omega = 0.3$  and  $\omega_c/\omega = 0.2$ . All the other quantities used in the analysis have been obtained by the above-mentioned parameters.

Figure 2 shows the variation of wave frequency with respect to the propagation vector ( $k$ ) for different values of spin-polarization ( $\eta$ ) in the absence of CE interaction ( $V_c = 0$ ). The solid, dashed, and dotted lines show the variation for fully polarized ( $\eta = 1$ ), partially polarized ( $\eta = 0.5$ ), and unpolarized ( $\eta = 0$ ) plasma, respectively. In this case, the dispersion decreases with increase in spin-polarization.

Figure 3 shows the variation of wave frequency with the propagation vector ( $k$ ) for different values of spin-polarization in the



**Fig. 3.** The variation frequency of the SPW ( $\omega$ ) with the propagation vector ( $k$ ) in the presence of CE interaction for the different values of the spin-polarization at  $\eta = 0, 0.5,$  and  $1,$  with  $B_0 = 1\text{T}$  and  $n_{0\alpha} = 10^{26}\text{ m}^{-3}$ .



**Fig. 4.** The variation of wave frequency ( $\omega$ ) with propagation vector ( $k$ ) for  $H = 0.1, B_0 = 1\text{T},$  and  $n_{0\alpha} = 10^{26}\text{ m}^{-3}$ .

presence of CE interaction. The solid, dashed, and dotted lines show the variation for fully spin-polarized ( $\eta = 1$ ), partially polarized ( $\eta = 0.5$ ), and unpolarized ( $\eta = 0$ ) plasma, respectively. The dispersion increases with increase in spin-polarization. The wave frequency for the fully spin-polarized case is about 21.5% more than that of unpolarized plasma at  $k \approx 1$ . This is due to the larger Fermi pressure under the influence of spin-polarization and spin magnetic moment of the electron which play a crucial role in the presence of the magnetic field.

Figure 4 shows the variation of wave frequency with the propagation vector. The solid line shows the variation in quantum plasma in the absence of spin-polarization ( $\eta = 0$ ), while the dashed line denotes the trend for classical plasma ( $\hbar = 0$ ). It is evident from the figure that the dispersion of SPW is more by about 15.8% in the quantum plasma due to the quantum diffraction effects.

Figure 5 shows the variation of power flow with frequency. The solid line shows the variation in the presence of CE effect and spin-polarization, the dotted line is for the absence of spin-polarization and the presence of CE effect, while the dashed line is for the absence of CE effect but in the presence of spin-polarization. It can be seen that with increasing values of  $\omega/\omega_0$ , the frequency decreases sharply. Furthermore, we observe that both the spin-polarization and the CE contributes to the power flow.

### Optical gain

We consider the conduction in the depletion region of a forward-biased p-n junction. The density states and occupation probability of electrons and holes in conduction and valance bands, respectively, are as follows:

$$\rho_{(e,h)}(E_{e,h}) = 4\pi(2m_{(e,h)}/\hbar)^{3/2}E_{(e,h)}^{1/2}, \tag{11}$$

$$f_{(e,h)}(E_{e,h}) = [\exp(E_{(e,h)} - E_{f_c})/k_B T + 1]^{-1}, \tag{12}$$

where  $E_e$  and  $E_h$  are measured from bottom of the conduction band and top of the valance band, respectively. In order to emit a photon with frequency  $\omega$ , the electron transits from the energy

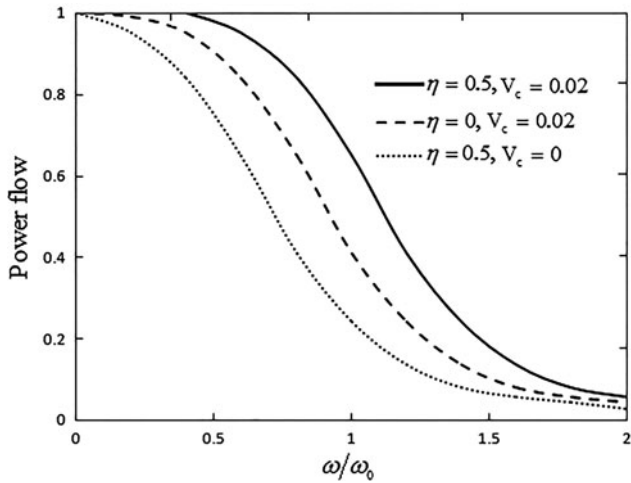


Fig. 5. The variation of power flow with  $\omega/\omega_0$  in the presence and absence of CE effect and spin-polarization, respectively, with  $H=0.1$  and  $n_{0\alpha}=10^{26} \text{ m}^{-3}$ .

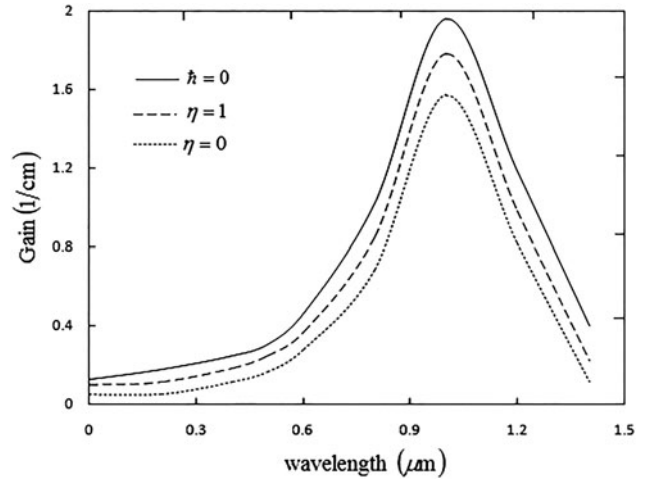


Fig. 6. The variation of the gain ratio with wavelength for spin-polarized quantum magnetoplasma for  $H=0.1$ ,  $B_0=1\text{T}$ , and  $n_{0\alpha}=10^{26} \text{ m}^{-3}$ .

state  $E_e$  (energy state of the conduction band) to the state  $E_h$  (energy state of the valance band) giving

$$\omega = \frac{E_e + E_h + E_g}{\hbar}, \tag{13}$$

where  $E_g$  is the bandgap. The propagation constant of the photon is much smaller as compared to that of the electron before or after the transition, hence in a direct bandgap semiconductor,

$$E_{(e,h)} = \frac{\hbar^2 k^2}{2m_{(e,h)}}. \tag{14}$$

For monochromatic SPW, the total energy produced per unit volume per unit second is  $W = \beta P_z$ , where  $\beta = \hbar \omega_0 B k \omega^{-1} \rho_e(E_e) \rho_h(E_h) [f_e(E_e) + f_h(E_h) - 1]$  is the amplification constant for the diode amplifier. Using Eqs. (7) and (9) together with Eq. (10) gives the net energy produced as

$$W = \beta' I, \tag{16}$$

where  $\beta' = 2\beta\omega/c \cdot \epsilon_1 \epsilon_2^2 e^{-2\alpha_1 d} / (\epsilon_1 - \epsilon_2) |\epsilon_1 + \epsilon_2|^3$  is the gain of SPW.

The ratio of the gains of SPW and diode amplifiers is

$$\frac{\beta' \Delta}{\beta} = \frac{2\omega \Delta \{(\epsilon'_L - \omega_{p\alpha j}^2 \cdot \omega) / (\omega^2 - k^2 Q_\alpha^2) - \omega_p^2 \omega m V_{cj}^2 / (\omega^2 - k^2 Q_\alpha^2)\} \cdot \{(\epsilon_L - \omega_p^2 / \omega)\}^2}{c \{(\epsilon'_L - \omega_{p\alpha j}^2 \cdot \omega) / (\omega^2 - k^2 Q_\alpha^2) - (\epsilon_L - \omega_p^2 / \omega)\} \cdot \{(\epsilon'_L - \omega_{p\alpha j}^2 \cdot \omega) / (\omega^2 - k^2 Q_\alpha^2) - \omega_p^2 \omega m_j V_{cj}^2 / (\omega^2 - k^2 Q_\alpha^2)\} + \{(\epsilon_L - \omega_p^2 / \omega)\}^3} e^{-2\alpha_1 d}, \tag{17}$$

Equations (13) and (14) define the energy states  $E_e$  and  $E_h$  that participate in the stimulated emission of radiation of frequency  $\omega$ . In the frequency interval  $\omega$  to  $\omega + d\omega$ ,  $u_\omega d\omega$  is the surface-plasmon energy density at the junction. The rate of electron-hole combination is proportional to the spectral density  $u_\omega$ . The rate of spontaneous emission and absorption resulting from the transition of electrons from conduction to the valance band and vice versa via photon emission and absorption are as follows:

$$R_{(st,abs)} = B u_\omega \rho_e(E_e) \rho_h(E_h) [f_e(E_e) f_h(E_h) \cdot \{1 - f_h(E_h)\} \cdot \{1 - f_e(E_e)\}] d\omega, \tag{15}$$

where  $B$  is Einstein's coefficient,  $f_e(E_e)$  is the occupation probability of state  $E_e$ , and the probability of state  $E_h$  being vacant is  $f_h(E_h)$ . For a higher value of the spectral density, the spontaneous emission can be ignored.

where  $\Delta$  is the width of the junction.

The variation of the gain ratio with wavelength is shown in Figure 6. The solid line denotes the trend for classical ( $\hbar = 0$ ), the dashed line denotes the trend for fully polarized plasma ( $\eta = 1$ ) for similar parameters, while the dotted line shows the trend in the absence of spin-polarization ( $\eta = 0$ ). The optical gain increases with increase in spin-polarization, attains maximum at about  $\approx 1.05 \mu\text{m}$ , where it is about 15% more than the non-polarized ( $\eta = 0$ ) case, and then falls off rather sharply. The spin-polarization becomes more significant at higher magnetic fields. The figure shows that the gain ratio is appreciably enhanced on the application of the external magnetic field. The gain ratio is reduced by about 12% in the limit  $\hbar \rightarrow 0$ , which is due to the quantum diffraction effects. This reduction in gain can be compensated by further increasing the magnetic field strength.

## Result and discussion

In the present study, the propagation of the surface plasma wave in magnetized quantum plasma incorporating the effects of the CE interaction and spin-polarization has been carried out. Using the QHD model with quantum corrections due to the Bohm potential, Fermi pressure, spin evolution, and exchange-correlation, a generalized dispersion relation is derived considering spin-up and spin-down electrons to be different species of particles. Spin effects are incorporated via spin force and macroscopic spin magnetization current. A dispersion relation for the SPW is derived and the gain ratio has been evaluated. In semiconductor quantum plasmas, the dispersion effects are due to the charge separation between the electrons and holes, the quantum recoil, the nonlinearities which arise due to large amplitude electrostatic potential, the quantum degeneracy pressure, and the CE interaction. It is found that the dispersion of the wave is slightly different from non-spin-polarized to fully polarized plasmas. The exchange interactions are used, based on the adiabatic local-density approximation and can be described as a function of the electron density. The contribution of spin-polarization with the CE interaction force becomes a crucial role with the increase in the external magnetic field. The magnetic field induces the difference between the population of spin-up and spin-down states which increases with magnetic field strength. Thus, the contribution of the CE interaction also becomes significant with an increase in the external magnetic field. The wave frequency is increased by 21.5% due to CE interaction than the absence of CE. The gain ratio of the SPW increases by 15.8% due to spin-polarization. These results may be important for ultra-small electronic devices or solid density plasmas, and understanding numerous collective phenomena in quantum plasmas. To be more specific the present study for surface-plasmon laser (SPASER) (Bergman and Stockman, 2003) and ultra compact biochemical sensors.

**Acknowledgment.** The work has been carried out under research project no. 39/14/12/2016-BRNS sanctioned by DAE-BRNS, India.

## References

- Agranovich VM (1975) Crystal optics of surface polaritons and the properties of surfaces. *Soviet Physics Uspekhi* **18**, 99–117.
- Andreev PA and Kuzmenkov LS (2016) Surface spin-electron acoustic waves in magnetically ordered metals. *Applied Physics Letters* **108**, 191605.
- Bergman DJ and Stockman IM (2003) Surface plasmon amplification by stimulated emission of radiation: quantum generation of coherent surface plasmons in nanosystems. *Physical Review Letters* **90**, 027402.
- Bozhevolnyi SI and Pudonin FA (1997) Two-dimensional micro-optics of surface plasmons. *Physical Review Letters* **78**, 2823–2826.
- Brodin G and Marklund M (2007a) Spin magnetohydrodynamics. *New Journal of Physics* **9**, 227.
- Brodin G and Marklund M (2007b) Spin solitons in magnetized pair plasmas. *Physics of Plasmas* **14**, 112107.
- Brodin G and Marklund M (2007c) Ferromagnetic behavior in magnetized plasmas. *Physical Review E* **76**, 055403.
- Brodin G and Marklund M (2008) On the possibility of metamaterial properties in spin plasmas. *New Journal of Physics* **10**, 115031.
- Goel D, Chauhan P, Varshney A and Sajal V (2016) Parametric excitation of surface plasma waves by stimulated Compton scattering of laser beam at metal-free space interface. *Laser and Particle Beams* **34**, 467–473.
- Homola J (1999) Surface plasmon resonance sensors. *Sensors and Actuators B: Chemical* **54**, 3–15.
- Homola J (2003) Present and future of surface plasmon resonance biosensors. *Analytical and Bioanalytical Chemistry* **377**, 528–539.
- Hong X and Kao FJ (2004) Microsurface plasmon resonance biosensing based on gold-nanoparticle film. *Applied Optics* **43**, 2868–2873.
- Hu QL, Linzhou S, Yu X and Cao R (2016) Spin effects on the EM wave modes in magnetized plasmas. *Physics of Plasma* **23**, 112113.
- Ishimaru A, Jaruwatanadilok S and Kuga Y (2005) Generalized surface plasmon resonance sensors using metamaterials and negative index materials. *Progress in Electromagnetics Research* **51**, 139–152.
- Kao WC, Chou C and Wu HT (2003) Optical heterodyne surface-plasmon resonance biosensor. *Optics Letters* **28**, 1329–1331.
- Kaw PK and McBride JB (1970) Surface waves on a plasma half-space. *Physics of Fluids* **13**, 1784–1790.
- Khorashadizadeh SM, Boroujeni ST, Rastbood E and Niknam AR (2012) Theoretical study of the surface waves in semi-bounded quantum collisional plasmas. *Physics of Plasmas* **19**, 032109.
- Kumar P, Tripathi VK and Liu CS (2008) A surface plasmon laser. *Journal of Applied Physics* **104**, 033306.
- Lazar M, Shukla PK and Smolyakov A (2007) Surface waves on a quantum plasma half-space. *Physics of Plasmas* **14**, 124501.
- Liu CS and Tripathi VK (2000) Excitation of surface plasma waves over metallic surfaces by lasers and electron beams. *IEEE Transactions on Plasma Science* **28**, 353–358.
- Manfredi G (2005) How to model quantum plasmas. *Fields Institute Communications* **46**, 263–287.
- Marklund M and Brodin G (2007) Dynamics of spin-1/2 quantum plasmas. *Physical Review Letters* **98**, 025001.
- Misra AP (2011) Electromagnetic surface modes in a magnetized quantum electron-hole plasma. *Physical Review E* **83**, 057401.
- Mohamed BF (2010) Quantum effects on the propagation of surface waves in magnetized plasma. *Physica Scripta* **82**, 065502.
- Moradi A (2017) Electrostatic surface waves on semi-bounded quantum electron-hole semiconductor plasmas. *Communications in Theoretical Physics* **67**, 317–321.
- Polyakov PA (1979) Hydrodynamic description of plasma waves including electron spin. *Soviet Physics Journal* **22**, 310–312.
- Rastunkov VS and Krainov VP (2004) Relativistic electron drift in overdense plasma produced by a superintense femtosecond laser pulse. *Physical Review E* **69**, 037402.
- Ritchie RH (1963) On surface plasma oscillations in metal foils. *Progress of Theoretical Physics* **29**, 607–609.
- Sahu B and Misra AP (2017) Magnetohydrodynamic shocks in a dissipative quantum plasma with exchange-correlation effects. *European Physical Journal Plus* **132**, 316.
- Shahid M, Melrose DB, Jamil M and Murtaza G (2012) Spin effect on parametric interactions of waves in magnetoplasmas. *Physics of Plasmas* **19**, 112114.
- Shahmansouri M (2015) The exchange-correlation effects on surface plasmon oscillations in semi-bounded quantum plasma. *Physics of Plasmas* **22**, 092106.
- Shahmansouri M and Mahmodi M (2017) Quantum electrostatic surface waves in a hybrid plasma waveguide: effect of nano-sized slab. *Physics of Plasmas* **24**, 102107.
- Shahmansouri M and Misra AP (2018) Surface plasmon oscillations in a semi-bounded semiconductor plasma. *Plasma Science and Technology* **20**, 025001.
- Shukla PK and Eliasson B (2007) Nonlinear interactions between electromagnetic waves and electron plasma oscillations in quantum plasmas. *Physical Review Letters* **99**, 096401.
- Trivelpiece AW and Gould RW (1959) Space charge waves in cylindrical plasma columns. *Journal of Applied Physics* **30**, 1784–1793.
- Yanovsky V, Chykov V, Kalinchenko G, Rosseau P, Planchon T, Matsuoka T, Maksimchuk A, Nees J, Cheriaux G, Mourou G and Krushelnick K (2008) Ultra-high intensity 300-TW laser at 0.1 Hz repetition rate. *Optics Express* **16**, 2109–2114.
- Zayats AA, Smolyaninov II and Maradudin AA (2005) Nano-optics of surface plasmon polaritons. *Physics Reports* **408**, 131–314.
- Zhu J (2015) Surface waves on the spin-1/2 quantum magnetoplasma half-space. *Journal of Plasmas Physics* **81**, 905810110.
- Zhu J, Zhao H and Qiu M (2013) Surface waves on the relativistic quantum plasma half-space. *Physics Letter A* **377**, 1736–1739.